(A Letter-of-Intent to Jefferson Lab PAC-44)

First Measurement of the $e - {}^3\vec{\text{He}}$ Parity Violating Deep Inelastic Scattering Asymmetry Using an Upgraded Polarized ^{3}He Target

K. Allada

.

R. Beminiwattha

Syracuse University, Syracuse, New York 13244, USA

F. Benmokhtar

Duquesne University, Pittsburgh, PA 15282, USA

A. Camsonne, J.-P. Chen, O. Hansen, W. Melnitchouk, and N. Sato

Thomas Jefferson National Accelerator Facility, Newport News, VA 23606, USA

G. D. Cates (co-spokesperson), K. Jin, J. Liu, K. Paschke,

V. Sulkosky, N. Ton, and X. Zheng (co-spokesperson)

University of Virginia, Charlottesville, VA 22904, USA

A. Deshpande, N. Feege, N. Hirlinger-Saylor, K. Kumar, T. Kutz,

S. Park, S. Riordan, and Y. X. Zhao (co-spokesperson and contact) [*]

Stony Brook University, Stony Brook, NY 11794, USA

H. Gao, X. Li, T. Liu, C. Peng, W. Xiong, X. Yan, and Z. Zhao

Duke University, Durham, NC 27708, USA

P. Markowitz

Florida International University, Miami, FL 33199, USA

A. W. Thomas

University of Adelaide, Adelaide SA 5005, Australia

[*] yuxiang.zhao@stonybrook.edu

Z. Ye

Argonne National Lab, Argonne, IL 60439, USA

Abstract

We propose here the first measurement of a parity-violating asymmetry between a unpolarized electron beam and a longitudinally polarized ^{3}He target in the deep inelastic scattering (DIS) region. In the DIS region, this single-target asymmetry is determined by the polarized electroweak interference structure functions $g_{1,5}^{\gamma Z}$ of the nucleon. With the known electron-quark effective neutral-weak couplings $C_{1q,2q}$, these polarized electroweak interference structure functions can be used to provide information on the spin structure of the nucleon, and further provide a test of the SU(3) flavor symmetry: the $g_1^{\gamma Z}$ term is approximately proportional to $\Delta\Sigma \equiv \sum_f(\Delta q + \Delta\bar{q})$, with Δq the polarized parton distribution function (PDF) and the summation is performed over all quark flavors; The $g_5^{\gamma Z}$ term is sensitive to the valence quark polarization $\Delta q_V \equiv \Delta q - \Delta\bar{q}$, including $\Delta s - \Delta\bar{s}$, that cannot be measured from existing methods such as double-polarized scattering or Drell-Yan measurements. For the kinematics proposed here, the $g_1^{\gamma Z}$ dominates the asymmetry. Therefore our primary goals are to provide a measurement on a new combination of the quark polarization Δq. By combining with double-polarization data on g_1^p and g_1^n, the contribution to the nucleon spin from the spins of the quarks, $\Delta\Sigma$, will be extracted for the first time without the use of the SU(3) flavor symmetry. In a similar manner, the SU(3) flavor symmetry can be tested for the first time.

We plan to used a 60-μA 11-GeV electron beam and the SoLID in Hall A to detect the scattered electrons in the inclusive mode. To control the trigger rate without impacting the physics outcome, only the large-angle detector package of SoLID will be used. The polarized ^{3}He target will be the 60-cm long cell with the metal end-windows expected from the stage-II upgrade, with an expected target polarization of 60%. In addition, two methods will be used to increase the density of the target chamber by a factor 16 compare to the present 12-amg density: First, fill pressure of the target cell will be increased by a factor 4, from 10 atm to 40 atm at the STP. Second, the target chamber will be cooled to liquid nitrogen temperature. The temperature difference between the pumping and the target chambers will cause a redistribution of the ^{3}He and another factor 4 increase in the target-chamber density. Both methods will require R&D should the proposed measurement moves forward. Our experimental setup is very similar to the approved $^3\vec{\text{He}}$ SIDIS measurements using SoLID with the exception of the increased target density. To form the single-

target asymmetry, the target spin direction will be flipped every minute.

We request 180 PAC days of beam time for the main production run. The measurement will cover wide ranges in x and Q^2. By combining different Q^2-bin data for the same x, within each x bin (with bin size $\delta x = 0.05$), the expected statistical uncertainty will be under 20% for the whole $x = (0.2, 0.75)$ range, and reach sub-10% for the four x bins between $x = (0.25, 0.45)$. It will provide the first measurement of the $g_{1,5}^{\gamma z}$ structure functions. By combining with the double-polarization $g_1^{p,n}$ data, the new data will provide the first test of the SU(3) flavor symmetry and to allow an extraction of $\Delta\Sigma$, the quark spin contribution to the nucleon spin, without the use of the SU(3) symmetry for the first time. The proposed measurement will also serve as an exporatory step for the $g_{1,5}^{\gamma Z}$ measurement planned for the future electron-ion collider (EIC).

Contents

1. MOTIVATION

1.1. The Physics of Polarized-Target PVDIS

For scattering of an unpolarized electron beam from a longitudinally polarized target, the asymmetry is parity-violating in nature. Details of the polarized PVDIS formalism are presented in Appendix A. To accentuate the physics, here we use the simplified form, derived from Ref. [1]:

$$A_{\text{pol-pvdis}} = \frac{\frac{d^2\sigma^{\Rightarrow}}{dx\,dy} - \frac{d^2\sigma^{\Leftarrow}}{dx\,dy}}{2\left(\frac{d^2\sigma}{dxdy}\right)_{\text{unpol}}} \approx \eta^{\gamma Z}\frac{f(y)g_A^e g_1^{\gamma Z}(x,Q^2) + g_V^e g_5^{\gamma Z}(x,Q^2)}{F_1^\gamma(x,Q^2)}, \tag{1}$$

where $\sigma^{\Rightarrow}$ and $\sigma^{\Leftarrow}$ are scattering cross sections with the target spin aligned parallel and anti-parallel to the beam direction, respectively; Q^2 is the negative of the four-momentum transfer squared, $x \equiv Q^2/(2M\nu)$ is the Bjorken scaling variable with M the nucleon mass; $f(y) = \frac{1-(1-y)^2}{1+(1-y)^2}$ with $y = \nu/E$, $\nu \equiv E - E'$ and E and E' are the initial electron and the scattered electron's energies, respectively; $g_{A,V}^e$ are the axial and the vector couplings of the electron; and

$$\eta^{\gamma Z} = \left(\frac{G_F M_Z^2}{2\sqrt{2}\pi\alpha}\right)\left(\frac{Q^2}{Q^2 + M_Z^2}\right). \tag{2}$$

Using the Fermi constant $G_F = 1.166 \times 10^{-5}$ (GeV)$^{-2}$ and the mass of the Z^0 $M_Z = 91.2$ GeV, we obtain $\frac{G_F M_Z^2}{2\sqrt{\pi}\alpha(Q^2+M_Z^2)} \approx \frac{G_F}{2\sqrt{2}\pi\alpha} \approx 180$ ppm/(GeV)$^{-2}$ and thus $\eta^{\gamma Z} \approx 180$ ppm/(GeV)$^{-2} \times Q^2$, with Q^2 in unit of GeV^2.

The structure function F_1^γ represents the unpolarized cross section and is given in the quark-parton model by the summation

$$F_1^\gamma(x) = \frac{1}{2}\sum_f e_{q_f}^2 q_f(x), \tag{3}$$

where $q_f(x)$ is the parton distribution function (PDF) of quark flavor f. Similarly, the electroweak interference (γZ) structure functions associated with a polarized target, $g_{1,5}^{\gamma Z}$, are

$$g_1^{\gamma Z} = \sum_f e_{q_f}(g_V)_{q_f}(\Delta q_f + \Delta \bar{q}_f) \tag{4}$$

$$g_5^{\gamma Z} = \sum_f e_{q_f}(g_A)_{q_f}, \tag{5}$$

where $(g_{A,V})_{q_f}$ are the axial and the vector couplings of the quark of flavor f. For the proton,

$$g_1^{p,\gamma Z} = \frac{2}{3}\left(\frac{1}{2} - \frac{4}{3}\sin^2\theta_W\right)(\Delta u + \Delta \bar{u} + \Delta c + \Delta \bar{c})$$

$$-\frac{1}{3}\left(-\frac{1}{2} + \frac{2}{3}\sin^2\theta_W\right)(\Delta d + \Delta \bar{d} + \Delta s + \Delta \bar{s}) \tag{6}$$

$$\approx \frac{1}{9}\left(\Delta u + \Delta \bar{u} + \Delta c + \Delta \bar{c} + \Delta d + \Delta \bar{d} + \Delta s + \Delta \bar{s}\right) \tag{7}$$

where the approximation is valid if we take $\sin^2\theta_W \approx 0.25$ with θ_W the weak mixing angle (the actual value is $\sin^2\theta_W = 0.235$). For the neutron:

$$g_1^{n,\gamma Z} = \frac{2}{3}\left(\frac{1}{2} - \frac{4}{3}\sin^2\theta_W\right)(\Delta d + \Delta \bar{d} + \Delta s + \Delta \bar{s})$$

$$-\frac{1}{3}\left(-\frac{1}{2} + \frac{2}{3}\sin^2\theta_W\right)(\Delta u + \Delta \bar{u} + \Delta c + \Delta \bar{c}) \tag{8}$$

$$\approx \frac{1}{9}\left(\Delta u + \Delta \bar{u} + \Delta c + \Delta \bar{c} + \Delta d + \Delta \bar{d} + \Delta s + \Delta \bar{s}\right) \tag{9}$$

$$\approx g_1^{p,\gamma Z} \tag{10}$$

Therefore each of $g_1^{p,\gamma Z}$ and $g_1^{n,\gamma Z}$ is approximately proportional to $\Delta\Sigma \equiv \Delta u + \Delta \bar{u} + \Delta c + \Delta \bar{c} + \Delta d + \Delta \bar{d} + \Delta s + \Delta \bar{s}$, the quark spin contribution to the nucleon spin. The $g_5^{\gamma Z}$ interference structure

functions are:

$$g_5^{p,\gamma Z} = \left[\frac{2}{3} \left(\frac{1}{2} \right) (\Delta u - \Delta \bar{u} + \Delta c - \Delta \bar{c}) - \frac{1}{3} \left(-\frac{1}{2} \right) (\Delta d - \Delta \bar{d} + \Delta s - \Delta \bar{s}) \right] \quad (11)$$

$$= \left[\frac{1}{3} (\Delta u_V + \Delta c - \Delta \bar{c}) + \frac{1}{6} (\Delta d_V + \Delta s - \Delta \bar{s}) \right] \quad (12)$$

$$g_5^{n,\gamma Z} = \left[\frac{1}{3} (\Delta d_V + \Delta s - \Delta \bar{s}) + \frac{1}{6} (\Delta u_V + \Delta c - \Delta \bar{c}) \right], \quad (13)$$

which can provide information on the valence quark's polarization, Δu_V, Δd_V and $\Delta s - \Delta \bar{s}$, that cannot be accessed from any other experimental methods.

Note that the single-target PVDIS asymmetry has a similar struture as the single-beam PVDIS asymmetry between a polarized beam and an unpolarized target [2, 3], which can be written as

$$A_{\mathrm{pvdis}} \approx \eta^{\gamma Z} \frac{g_A F_1^{\gamma Z}(x, Q^2) + f(y) g_V F_3^{\gamma Z}(x, Q^2)}{F_1^{\gamma}(x, Q^2)}. \quad (14)$$

Comparing Eq. (1) with Eq. (14), we note three distinct features: First, in Eq. (1) the y-dependence appears in the $g_A^e g_V^q$ ($g_1^{\gamma Z}$) term, which means the electron's parity-violating term is kinematically suppressed. This is opposite to the single-beam PVDIS asymmetry Eq. (14) where the quark parity-violation $g_V^e g_A^q$ ($F_3^{\gamma Z}$) term is kinematically suppressed. Second, the $g_A^e g_V^q$ ($g_1^{\gamma Z}$ or $F_1^{\gamma Z}$) term is the dominant term of the asymmetry in both cases because of the small value of g_V^e. Third, the size of the $g_1^{\gamma Z}$ is always smaller than $F_1^{\gamma Z}$ because of the suppression from quark polarization ($\Delta q/q < 1$). The single-target PVDIS asymmetry $A_{\mathrm{pol-pvdis}}$ [Eq. (1)] is thus always smaller in magnitude than the single-beam PVDIS asymmetry [Eq. (14)], and is more difficult to measure precisely. (In the following sections we will see that the use of polarized ^{3}He as an effective polarized neutron target decreases the size of the asymmetry even further. But this is unavoidable due to the lack of high-density polarized nucleon targets.)

1.2. SU(3) Symmetry and the Proton Spin Puzzle

There exist two sum rules for decomposing the proton spin [4]: The Jaffe-Manohar sum rule

$$\frac{1}{2} = \frac{1}{2} \Delta \Sigma + l_q^z + \Delta G + l_g^q \quad (15)$$

where the individual terms are the spin and orbital angular momenta (OAM) of the quark and gluon partons. The Ji sum rule states

$$\frac{1}{2} = \frac{1}{2} \Delta \Sigma + L_q^z + \Delta G + J_g^q \quad (16)$$

where J_g^q is the total angular momentum from the gluon. The difference between the two sum rules comes from the argument that the gluon J_q^q term may not be gauge-invariantly decomposed into its spin and OAM. The two sum rules, on the other hand, refer to the same decomposition for the quark contribution to the nucleon spin, that it can be separated into the contribution from the quark spin $\Delta\Sigma$, and the quark OAM L_q^z.

Existing parameterizations of the polarized PDF are based on two kinds of data: inclusive DIS using different lepton beams and nuclear targets; and Drell-Yan experiments. From inclusive DIS, flavor decomposition can be done by combining data from different nuclear targets. Typical observables are the g_1 polarized structure functions, which in the parton model can be written as:

$$g_1^P = \frac{1}{2}\left(\frac{4}{9}(\Delta u + \Delta\bar{u}) + \frac{1}{9}(\Delta d + \Delta\bar{d}) + \frac{1}{9}(\Delta s + \Delta\bar{s})\right), \qquad (17)$$

$$g_1^n = \frac{1}{2}\left(\frac{1}{9}(\Delta u + \Delta\bar{u}) + \frac{4}{9}(\Delta d + \Delta\bar{d}) + \frac{1}{9}(\Delta s + \Delta\bar{s})\right), \qquad (18)$$

where the isospin symmetry ($u^p = d^n$, $d^p = u^n$, and $s^p = s^n$) has been applied for the polarized PDF. However, the nucleon g_1 data provide only two conditions. Unless if we can find a third kind of nucleon (in addition to the proton and the neutron), for a full decomposition into three flavors u, d, s, the SU(3) flavor symmetry must be used as a third constraint. In naive quark models, once the SU(3) flavor symmetry is assumed, the knowledge from the β decays of the neutron and the hyperons can be combined with the first moment (Γ_1) of g_1 to determine the spin-flavor decomposition. The β-decay constants determine the octet parts of the flavor contributions ($g_A^{(8)} = \Delta u + \Delta d - 2\Delta s$) and, together with Γ_1, can be used to reveal the value of the flavor singlet contribution $\Delta\Sigma$ (also written as $g_A^{(0)} = \Delta u + \Delta d + \Delta s$), the total quark contribution to the proton spin. (For a review of the current status of spin structure functions, please see, e.g. Ref. [5]). Another method of flavor decomposition of the nucleon spin, without relying on the SU(3) symmetry, is to use Drell-Yan data. However, interpreting Drell-Yan data depends on models for fragmentation functions.

The current value for $\Delta\Sigma$ is determined from experiements [6] as:

$$\Delta\Sigma = 0.33 \pm 0.03(\text{stat.}) \pm 0.05(\text{syst.}), \qquad (19)$$

along with a large strange quark polarization $\Delta s \approx -0.12$. As mentioned in previous paragraphs, flavor decomposition from inclusive data alone is impossible without the use of the flavor SU(3) symmetry. However, SU(3) symmetry has never been tested experimentally. In recent theoretical

work, it has been shown that the SU(3) symmetry can be broken at a level as much as 20% [7]. The proposed measurement will provide direct and model-independent data for $\Delta\Sigma$. And by combining this unique result with data on $g_1^{p,n}$, the SU(3) symmetry can be tested for the first time.

2.   EXPERIMENTAL SETUP

2.1.   The Electron Beam

We will use an 11-GeV electron beam with a current of 60 μA. If the beam is longitudinally polarized, the PVDIS event counts will be summed over the two beam helicity states to form the single-target PVDIS asymmetry. Because transverse polarization of the beam can be a systematic background to the measurement, we require the transverse polarization of the beam to be mini-mized ("null-ed") using the stardard parity-violation experiment technique, regardless of what the longitudinal polarization will be. Due to the use of the polarized ^{3}He target, the beam must be rastered to a large cross-sectional area, of at least 4×4 mm^2 in size. The use of the polarized beam could possibly provide control measurements parasitically to the main asymmetry measurement. This will be worked out if we pursue a full proposal.

2.2.   The Polarized ^{3}He Target

The JLab polarized ^{3}He target utilize the optical pumping spin-exchange method: the target cell is filled with high-pressure ^{3}He mixed with a small amount of alkali metal such as Rb and K. A high-power laser is used to optically-polarize the Rb (or K) atom, then the Rb atoms transfer their polarization to the ^{3}He nuclei through spin-exchange during their collisions. A small amount of (unpolarized) N$_2$ is usually mixed with the ^{3}He gas to minimize the emission of (unpolarized) light from immediate de-excitation of the Rb. The best target performance achieved by the JLab's 6 GeV program is a luminosity of 1.2×10^{36} neutrons/sec/cm^2, provided by a 12-amg density, 40-cm target length, 15-μA beam current, and a 55% target polarization.

There have been many experiments approved for the JLab 12 GeV program that utilize the po-larized ^{3}He target, most requiring an upgrade to the luminosity. The target upgrade is by far being planned as two stages, both being carried out at the University of Virginia by the group of Prof. Gordon Cates. Compare to the best 6 GeV performance, the stage-I target upgrade is aiming for

a 60% polarization, 40-cm target length and a 30-μA beam current (2.4×10^{36} neutrons/sec/cm^2), realized via the use of narrow-band lasers, hybrid pumping, and a convection-type cell design. The stage-II upgrade, as proposed by the (12 GeV) GEn-II collaboration [8], will achieve a 60% polarization, 60-cm target length and a 60-μA beam current (7.2×10^{36} neutrons/sec/cm^2) by increasing the laser power and enlarging the target pumping chamber from 2.2 to 3 liters, and by adding metal end-windows to the target chamber to accommodate the higher beam current. The target density will remain the same 12 amg for both stages. An R&D cell for the GEn-II target is shown in Fig. 1, which has accommodated all proposed upgrades except the larger (3-liter) pumping chamber and the metal end windows.
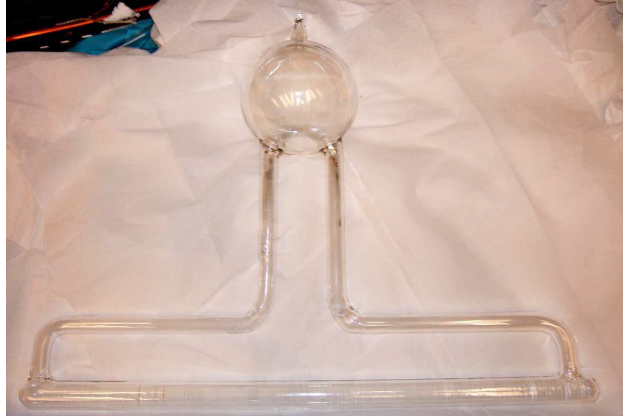

FIG. 1: From Ref. [8], the first prototype "convection-driven" target cell. Made entirely out of glass, this cell approximates the geometry of the proposed GEN-II target-cell geometry and is being used to prove the concept of mixing the gases of the pumping chamber and target chamber using convection.

For this proposal, we plan to use the stage-II target and with a factor 16 increase in the target chamber density, reaching approximately 10^{38} neutrons/sec/cm^2. The density increase can be done by filling the target with 40-atm pressure (at STP this provides a 40-amg density) instead of the current 10 atm, and by cooling the target chamber in liquid nitrogen during the run. The LN$_2$ cooling will redistribute the ^{3}He and increase the target-chamber density by another factor 4.

The density redistribution due to the temperature gradient is straightforward to calculate as follows: If the density of the cell is n_0 when the whole cell is at the same temperature, and under running conditions the pumping chamber is raised to a temperature T_p while the target chamber is

lowered to T_t, the densities in the two chambers are [9]:

$$n_P = \frac{n_0}{1 + \frac{V_T}{V_0}\left(\frac{T_P}{T_T} - 1\right)} \tag{20}$$

$$n_T = \frac{n_0}{1 + \frac{V_P}{V_0}\left(\frac{T_T}{T_P} - 1\right)} \tag{21}$$

where V_P, V_T are volumes of the pumping and the target chambers, respectively, and $V_0 = V_P + V_T$ if ignorning the volume of the transfer tube. For existing 6-GeV targets which operated at approximately $T_P = 230°\text{C}$ and $T_T = 50°\text{C}$, the target-chamber density usually reaches 11 to 12 amg. For a cell with $V_P = 3$ liter (stage-II geometry), $V_T = 0.188$ liter assuming the target chamber is a 1-cm radius, 60-cm long cylinder; $T_P = 230\ °\text{C}$ and $T_T = 77\ \text{K}$ provided by the liquid-nitrogen cooling; and assuming a fill pressure of 40 atm at the STP (40 amg density), the densities reach

$$n_P = \frac{n_0}{1 + \frac{0.2\ \text{liter}}{3.2\ \text{liter}}\left(\frac{500\text{K}}{77\ \text{K}} - 1\right)} = 0.744 n_0 = 29.8\ \text{amg}, \tag{22}$$

$$n_T = \frac{n_0}{1 + \frac{3.0\ \text{liter}}{3.2\ \text{liter}}\left(\frac{77\text{K}}{500\text{K}} - 1\right)} = 4.83 n_0 = 193\ \text{amg}, \tag{23}$$

which is at least a factor 16 increase in density compare to the 12 amg of the stage-II target. The resulting pressure in the two chambers are

$$P_P = n_P R T_P = P_T = n_T R T_T = 54\ \text{atm}. \tag{24}$$

Both methods described above to increase the target-chamber density will require dedicated R&D if the proposed measurement moves forward. It is worth noting that pressurized ^{3}He and ^{4}He (unpolarized) targets used by the early SLAC-NA9 experiment operated at a pressure of 50 atm [10], therefore at least one of the two methods has been (somewhat) utilized previously. One missing ingredient, which will probably be crucial, is to increase the ^{3}He circulation between the two chambers to quickly replace the ^{3}He depolarized by the high beam current. The convection-type circulation alone may not be fast enough for the new target density design. Another R&D item will be how the metal end windows and the metal-glass junction can hold the 4 times higher pressure. On the other hand, the low temperature of the target chamber may help with increasing the spin-relaxation time T_1 of the cell, since existing data indicates that lowering the temperature with liquid nitrogen can significantly increase T_1 compared to room temperature.

2.3. The Solenoid Large Intensity Device (SoLID)

The SoLID (Solenoidal Large Intensity Device) [11] is a large acceptance spectrometer capable of handling very high rates with a large acceptance. It is designed for five approved experiments and will become one of the base equipment for the 12 GeV program in experimental Hall A. It has two configurations to accomodate two kinds of experiments: the "SIDIS" (Semi-Inclusive Deep Inelastic Scattering) and the PVDIS configurations. We plan to use the same detector setup as the SIDIS configuration for our measurement with the target length changed from 40 cm to 60 cm, and we will focus on using the large-angle detectors.

A schematic view of the SoLID SIDIS configuration is given in Fig. 2. The spectrometer will be built based on the CLEO solenoidal magnet. The detector setup we propose to use is identical to that of SIDIS experiments E12-10-006 [12] and E12-11-007 [13]. Per design for SIDIS processes, the detector system consists of forward-angle detectors with a polar angle coverage from 6.6 to 12 degrees and large-angle detectors with a polar angle coverage from 13 to 22 degrees. For the proposed measurement, because of the increased luminosity, we plan to detect inclusive electrons in only the large-angle detectors where the single-electron rates are low enough to be accommodated by the existing data acquisition (DAQ) system.
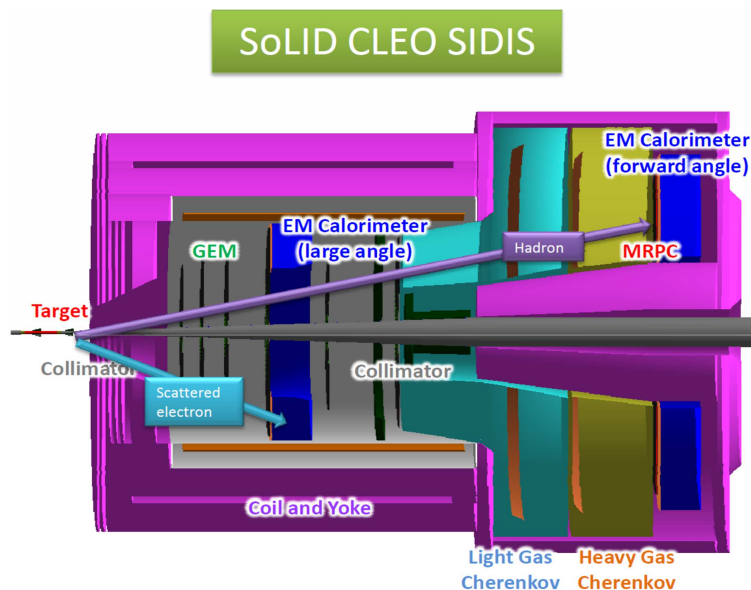

FIG. 2: SoLID detector setup for the SIDIS configuration. For the proposed measurement we will focus on using the large-angle detectors.

Six layers of GEM detectors will be placed inside the CLEO coils as tracking detectors for both regions. It is used to determine the momentum, angle and vertex of the charged particles. The forward-angle detector system will see five layers of GEM detectors while the large-angle detector system will see four layers of GEM detectors. The GEM detectors have a so-called "COMPASS design" which can handle a flux as high as 30 kHz/mm^2. We expected the following approximate performance from GEM: spatial resolution 200 μm, average momentum resolution 1.2%, polar-angle resolution 0.3 mrad, azimuthal-angular resolution 6 mrad, and an average vertex resolution of 0.8 cm. The SoLID collaboration has built a prototype of GEM detector with its size similar to one sector module in a disk layer configuration of GEM planes in SoLID. The prototype is also tested at Fermilab and the results are promising as shown in [14].

The large-angle detector package consists of an electromagnetic calorimeter (ECal) and a thin layer of scintillator pad detector (SPD) to reject photons. (The SPD has the same lateral coverage as the ECal and is placed immediately in front of the ECal. The SPD is not shown in Fig. 2). The ECal is longitudinally segmented into a preshower and a "shashlyk"-type shower. For SIDIS experiments, the ECal alone is sufficient for electron identifications. For the proposed measurement, although we will detect DIS electrons in the inclusive mode where photo- and electro-produced pions are often the major background, the expected statistical uncertainty is large, and thus the ECal alone is considered sufficient for PID.

3. SIMULATIONS AND EXPECTED RESULTS

3.1. SoLID Simulations

The GEMC [15] was employed as simulation tool for our rate estimations. It was successfully developed and used for the CLAS12 collaboration. It utilizes GEANT4 and includes facilities for external event generators. The SoLID simulation group has successfully incorporated all the necessary SoLID detector geometry in GEMC, and provided simulation for all SoLID experiments [11]. The rate information presented in this document was simulated by inheriting the GEMC SIDIS configuration from E12-10-006 and E12-11-007 but with the polarized ^{3}He target length modified from 40 to 60 cm.

3.2. Rate and Asymmetry Calculations

The kinematic coverage of the large-angle detector package is shown in Fig. 3 as a function of x and Q^2. The rates are shown in Fig. 4.
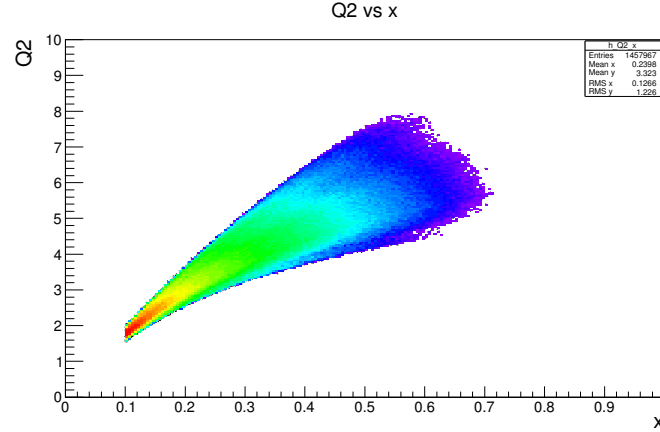

FIG. 3: The (x, Q^2) kinematic coverage of the large-angle detector package of SoLID, simulated for inclusive electrons with an 11 GeV electron beam on a 60 cm long polarized ^{3}He target.

The asymmetry for different (x, Q^2) bins were calculated using Eqs.(1-2), with the structure functions calculated using the quark parton model, Eqs. (3), (6), (8), (12) and (13). LHAPDF6 [16] was employed as an interface to access both polarized and unpolarized PDFs needed for the calculation. The latest version of LHAPDF6.1.6 was used. The unpolarized PDFs accessible through LHAPDF6 include CT and MRST-MSTW-MMHT. We focused on using CT14NLO. For the unpolarized PDF, however, the only set available through LHAPDF6 is NNPDF [17]. More polarized PDF sets such as LSS2010 [18], BB2010 [19], and DSSV2008 [20, 21] were explored but we did not find sizable differences in the calculated asymmetry compared to NNPDF. In the future, we also plan to employ local resources at JLab and include the most recent CJ15 [22] and JAM15 [23] for the unpolarized and the polarized PDF choices, respectively. In addition, we are working with the JAM Collaboration to evaluate possible impact of the expected results from this measurement on the understanding of the nucleon spin and polarized PDF. This will be discussed in Section 5.

Once the proton and the neutron asymmetries were obtained, the ^{3}He asymmetry was calculated as [24, 25]

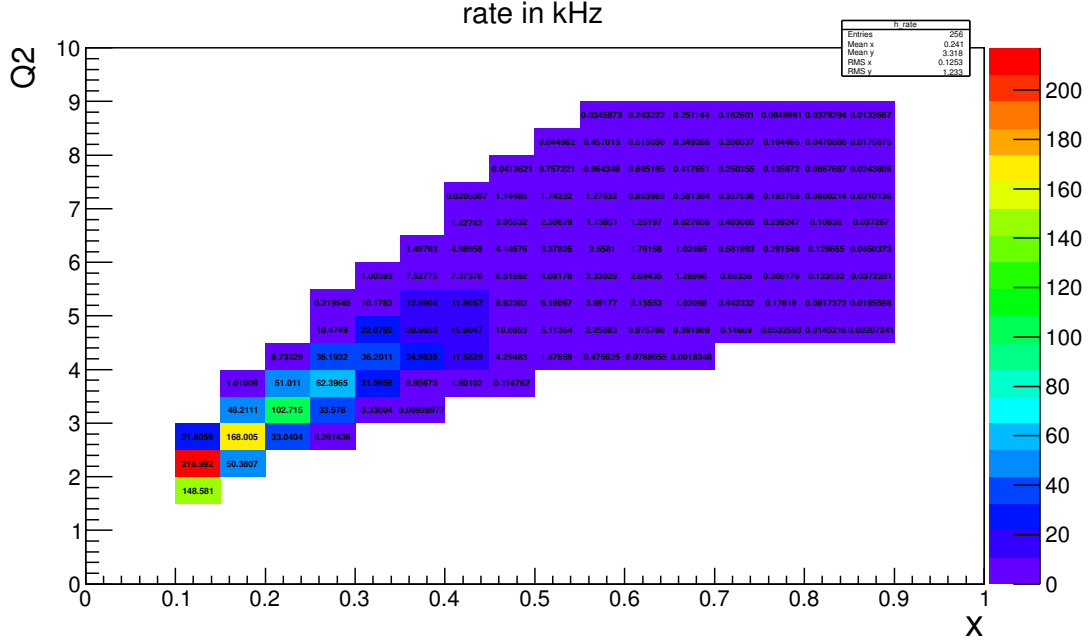$$A_{^3\text{He}} = P_n(1 - f_p)A_n + P_p f_p A_p, \tag{25}$$

FIG. 4: Rate simulated for the large-angle detector package of SoLID in (x, Q^2) bins. An 11 GeV, 60 μA beam was used in the simulation, and the target simulated is 60-cm long with the 193-amg density proposed in section 2.2.

where $P_n = 0.86^{+0.036}_{-0.02}$ and $P_p = -0.028^{+0.009}_{-0.004}$ are effective polarizations of the neutron and the proton in a polarized ^{3}He, respectively; $f_p = \frac{2\sigma_p}{\sigma_{3\,\mathrm{He}}}$ is the proton dilution factor with σ the unpolarized cross section for the proton or ^{3}He. We note that compare to the PVDIS asymmetry between a longitudinally polarized beam and an unpolarized target, the single-target PVDIS asymmetry is smaller because the quarks are not fully polarized in the nucleon ($|\Delta q/q| < 1$). The asymmetry is reduced further for ^{3}He because of the dilution from the two extra protons.

The ^{3}He asymmetries for different (x, Q^2) bins are shown in Fig. 5. In the bottom panel of the same figure, we show the uncertainty of this calculation using the eigenfunction sets of NNPDF-pol11 [26].

Assuming 180 days of beam time, the raw asymmetry can be formed from the measurement as

$$A_{\mathrm{raw}} = \frac{N^\Rightarrow - N^\Leftarrow}{N^\Rightarrow + N^\Leftarrow} \tag{26}$$

where $N^\Rightarrow$ and $N^\Leftarrow$ are the inclusive electron counts measured when the target spin is parallel and
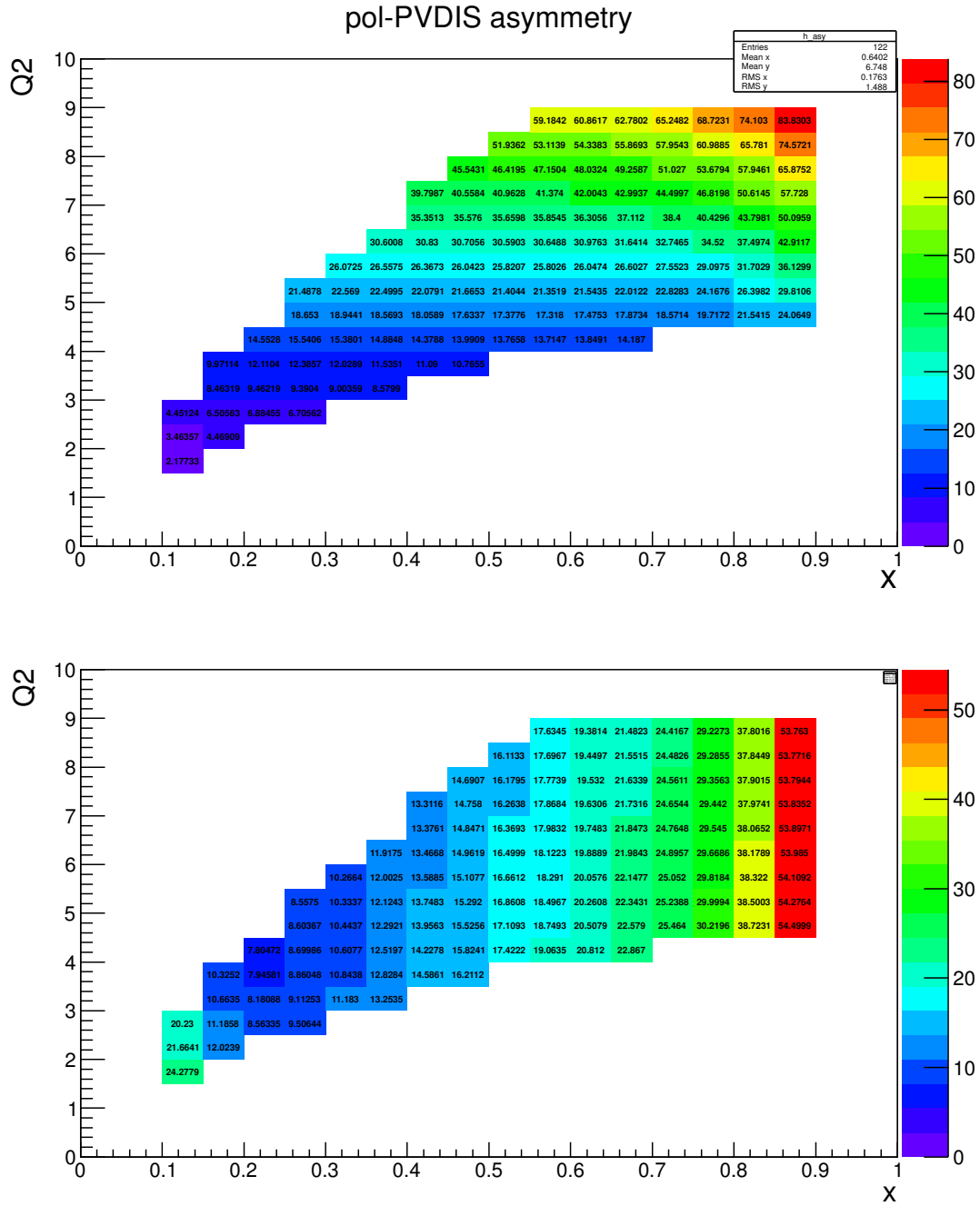
pol-PVDIS asymmetry

FIG. 5: *Top:* Calculated parity-violating asymmetries between an unpolarized beam and a polarized ^{3}He target, in ppm, for the kinematic coverage of the large-angle detector package of SoLID. The calculation was done by using CT14nlo for the unpolarized PDFs and NNPDFpol11 for the polarized PDFs. *Bottom:* Relative uncertainties for the calculated asymmetry, in percent, using the NNPDFpol11 PDF eigenfunction sets.

antiparallel to the beam direction, respectively. The uncertainty in the raw asymmtry is

$$\Delta A_{\text{raw}} = \frac{1}{\sqrt{N^{\Rightarrow} + N^{\Leftarrow}}}, \tag{27}$$

where the denominator can be calculated using the rate simulated from GEMC and the proposed beam time. To calculate the physics asymmetry for ^{3}He, we correct the raw asymmetry by the 60% target polarization and a dilution factor due to the small amount of N_2 in the target. From previous DIS measurements using the polarized ^{3}He target [24, 25], the N_2 dilution was typically 0.10 or less, giving a 0.90 correction factor:

$$\Delta A_{\text{phys}} = \frac{\Delta A_{\text{raw}}}{0.60 \times 0.90}. \tag{28}$$

Therefore, the relative uncertainty on the ^{3}He asymmetry can be estimated as

$$\frac{\Delta A_{^3\text{He}}}{A_{^3\text{He}}} = \frac{\Delta A_{\text{phys}}}{A_{^3\text{He}}} = \frac{\Delta A_{\text{raw}}}{0.60 \times 0.90 A_{^3\text{He}}}, \tag{29}$$

where $A_{^3\text{He}}$ is the ^{3}He asymmetry calculated from PDF sets using Eq. (29).

The expected statistical uncertainty for the ^{3}He asymmetry using the large-angle detector package of SoLID are shown in Fig. 6. The uncertainty can be reduced if data from different Q^2 bins are combined for the same x, reaching possibly $< 10\%$ for the $x < 0.5$ region. On the other hand, the estimation here used all the DIS electrons with $Q^2 > 1$ (GeV/c)^2 and $x > 0.1$, and did not assume any hardware threshold or trigger cuts.

To investigate the effect from hardware cuts on the measurement, we studied two possible cuts that can be employed in the detector and the trigger setup: one is a momentum $p > 3$ GeV/c cut that can be applied by setting a fixed threshold on the ECal; the other is a $Q^2 > 3$ (GeV/c)^2 cut that can be applied by setting a radial-dependent threshold on the ECal. The effect on the measured statistical uncertainty is shown in Fig. 7. As one can see, a radial-dependent trigger cut that corresponds to $Q^2 > 3$ (GeV/c)^2 has minimal effect on the measurement, and the combined statistical uncertainty can be as low as (9-10)% for the four x bins between 0.25 and 0.45. Because the asymmetry is dominated by the $g_1^{\gamma Z}$ ($> 90\%$ contribution), the proposed measurement will therefore provide a direct and model-independent information on $\Delta\Sigma$, the quark spin contribution to the nucleon spin, at the same sub-10% level.
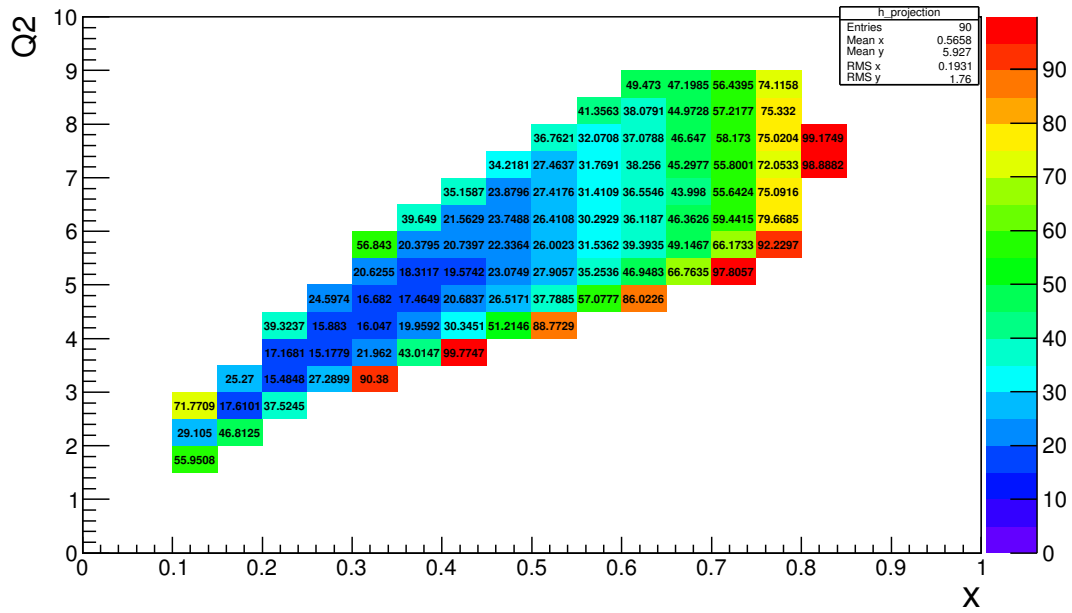
FIG. 6: Expected statistical uncertainty on the ^{3}He single-target PVDIS asymmetry, $\Delta A_{3\text{He}}/A_{3\text{He}}$ in percent, for the large-angle detector package of SoLID. The beam time used is 180 days. Corrections due to a 60% target polarization and a 0.90 N_2 dilution factor have already been applied.
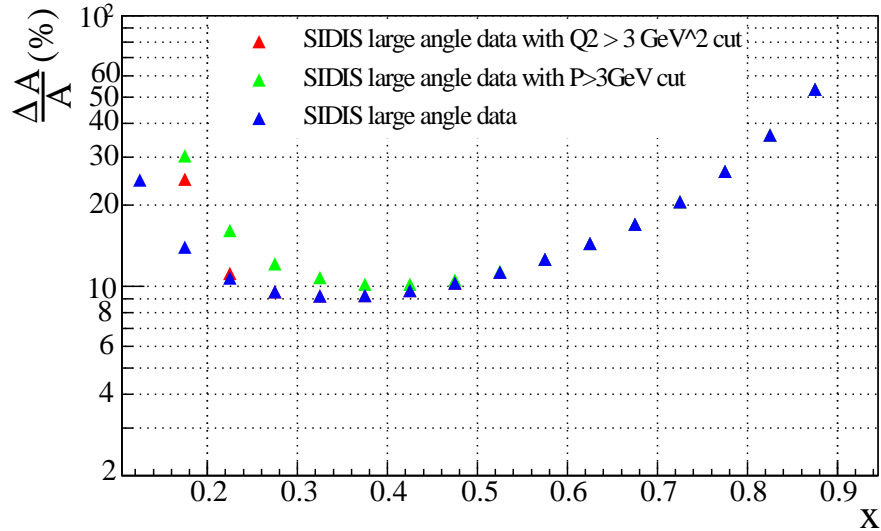

FIG. 7: Expected statistical uncertainty on the ^{3}He single-target PVDIS asymmetry, $\Delta A_{3\text{He}}/A_{3\text{He}}$ in percent, for the large-angle detector package of SoLID using different hardware shreshold and/or trigger cuts. Data from different Q^2 bins were combined to reduce the statistical uncertainty.

3.3. Trigger Rates and Backgrounds

We follow the trigger design of the SIDIS experiments E12-10-006 and E12-11-007, but only require the large-angle electron trigger for the proposed measurement. For the large-angle detectors, the electron triggers are formed from the ECal and the SPD. A $p > 3$ (GeV/c) trigger cut on the particle momentum can be applied by requiring a flat threshold on the large-angle ECal, yielding a trigger rate of about 2.2 MHz for the large-angle detector. If we assume 30 segmentations on the detector set-up, the trigger rate will be 73.3 kHz/sector, which is within the design parameters of the current DAQ of SoLID.

Simulations for a $Q^2 > 3$ (GeV/c)^2 cut is underway. This will likely yield a higher trigger rate. At the meantime, it is expected that the DAQ rate limit will be improved by the use of APV25 readout. It is also possible to reduce the trigger rate by modifying the GEM since the proposed measurement will make use of the large-angle data only. This will be worked out if we move forward with a full proposal.

For the offline electron identifications, the combination of preshower and shower for the ECal can provide a pion rejection facor of $200 : 1$ at $E > 3.5$ GeV and $100 : 1$ at $E > 1.0$ GeV. The pion background will thus have a $< 1\%$ systematic effect on the measured asymmetry, an order of magnitude smaller than the expected statistical uncertainty. Thus if we use only the large-angle detector package, the particle-identification using ECal alone is considered sufficient for the proposed measurement.

4. SYSTEMATIC UNCERTAINTY OF THE MEASUREMENT

In this section we investigate possible systematics effects on the measurement. Overall, these effects are found to be small compared to the expected statistical uncertaity.

4.1. Kinematic Reconstruction (Q^2)

In order to extract the $g_1^{\gamma Z}$ structure function out of the measured asymmetry, one needs to know the precise information of Q^2 for each event. Hence, we will need precise measurements of the beam energy, the scattering angle and the final-state particle energy. Measurements of beam energy can be better than 10^{-3} accuracy at JLab. With high-resolution GEM tracking information

and sufficient knowledge of the magnetic field in the tracking area, the scattering angle is expected to be about 0.5 mrad accuracy (E12-10-007) [13]. The SIDIS experiments (E12-10-006 and E12-11-007) [12, 13] will have sufficient calibration runs using elastic scattering off hydrogen at beam energies of 4.4 and 6.6 GeV to calibrate the particle momentum as well as Q^2. Overall, we expect the Q^2 measurement to be at a $\approx 0.2\%$ accuracy. Moreover, since we plan to use SIDIS detector configuration for our measurement, we can employ ep coincidence processes to select pure elastic events to improve Q^2 calibration.

4.2. Radiative Corrections

Due to the photon emission for the incident and the scattered electrons, the measured kinematics such as x, Q^2 have slight shifts compared to the quantities at the reaction vertex. Hence, radiative corrections should be applied to the measured asymmetries. The theory for the EM radiative correction is well developed and the corrections can in principle be calculated. The correction uncertainty arises from the uncertainty of the input structure functions. To control the uncertainty of the EM radiative correction, we can rely on both parameterizations and direct measurements. We can measure parasitic inclusive electron data from a longitudinally polarized ^{3}He target in E12-11-007 in a broad kinematic range. In addition, it is worth noting that during the 6 GeV $\vec{e}-^2$H PVDIS experiment, the PV asymmetry measured in the nucleon resonance region was in good agreement with calculations using DIS PDF parametrizations extrapolated to the resonance region [27], indicating that the quark-hadron duality to be valid for electroweak interference structure functions. We expect the radiative correction uncertainty to be about 0.3%.

4.3. Target Polarimetry

The relative uncertainties on polarimetry is expected to be 3% for the ^{3}He target. This will yield a 3% relative uncertainty to the measured asymmetries.

4.4. Contributions from $g_5^{\gamma Z}$

The measured parity-violating asymmetry proposed is $> 90\%$ dominated by $g_1^{\gamma Z}$, with the remaining $< 10\%$ contribution from $g_5^{\gamma Z}$. To extract $g_1^{\gamma Z}$ and set a contraint on $\Delta\Sigma$ and the test of

the SU(3) flavor symmetry, one has to subtract the $g_5^{\gamma Z}$ contribution from the asymmetry. The $g_5^{\gamma Z}$ structure function has never been measured before, therefore we need to rely on calculations using PDF fits. The uncertainty of the $g_5^{\gamma Z}$ from PDF fits is at about 5%. This gives a 0.5% relative uncertainty to the extracted $g_1^{\gamma Z}$.

4.5. Nuclear effects of ^{3}He

As discussed in the previous section, the ^{3}He asymmetry is extracted using effective nucleon polarizations in the ^{3}He wavefunction, Eq. (25). The uncertainty in the effective polarizations, $P_n = 0.86^{+0.036}_{-0.02}$ and $P_p = -0.028^{+0.009}_{-0.004}$, gives an uncertainty in the ^{3}He asymmetry calculation. For most of the kinematic region covered by the proposed measurement, the relative uncertainty in the calculated ^{3}He asymmetry due to the uncertainties of $P_{p,n}$ is between $(3-5)\%$.

4.6. Beam Related Systematic Uncertainties and Target Spin Flip Frequency

The measured raw asymmetry is given by Eq. (26). In practice, the beam current and trajactory are not exactly the same for two spin states. The charge correction as well as corrections related to beam position, beam angle etc. should also be performed:

$$A_{\text{meas}} = A_{\text{raw}} - A_{\text{Charge}} - \sum \alpha_i (\Delta X_i), \tag{30}$$

where $\alpha_i \equiv \partial\sigma/\partial X_i$, X_i is the beam parameters like beam position, σ is the physical cross section, ΔX_i is the beam fluctuation within the period of a target "spin pair". The extracted measured asymmetry A_{meas} is then used in place of A_{raw} when extracting the physics asymmetry from the measurement using Eq. (28.

Unlike the case of the measurement of beam helicity flip asymmetry (as measured in SoLID PVDIS for example), there is not any expected significant systematic error to be introduced in the grand average A_{mea} due to false asymmetries in the beam properties when the target's longitudinal polarization is reversed. However, additional random noise might be introduced due to beam trajectory fluctuations, which would result in significantly longer beam time requirements to achieve the required statistical errors. In the following paragraph, we outline the technical challenge that must be overcome to ensure that the asymmetry measurement will be dominated by statistical fluctuations.

It is proposed to flip the target helicity pseudo-randomly once every minute i.e. one constructs the various terms in Eq. (30 for each target "spin pair", where a pair contains the difference in each observable (detector counts and beam parameters) with respect to target spin flip over a period of 2 minutes. Neglecting beam fluctuations and in the limit of perfect detector and monitor resolution, A_{meas} should reflect the counting statistics in the scattered electron rate over a period of 2 minutes.

In order to explore the beam stability and monitoring resolution required to achieve counting statistics, we chose the (x, Q^2) bin with the highest rate, which is about 200 kHz. The counting statistics over a 2 minute period in this bin is 2.4×10^7 which implies that A_{meas} should have a variance of about 200 ppm. This implies that each of the corrections on the right hand side of Eq. (30) must be made with a resolution that is of the order of 20 ppm so as not to degrade the 200 ppm width significantly. For example, the integrated beam current fluctuations over one-minute time windows should be stable at the level of 1000 ppm, and the charge monitor resolution over the same duration should be of order 10 ppm. Likewise, the beam position should be stable at the level of 100's of microns and the position resolution over one-minute durations should be of the order of a few microns. Simulations will be carried out in order to improve the estimations for the specific configuration of the proposed measurement.

Experience during the PVES program in the 6 GeV era indicated that these criteria will be met, primarily due to the extraordinary stability of the CEBAF beam and the development of beam monitors with the required resolution to carry out previous PVES experiments. It is planned to study the beam and monitor fluctuations over one minute time scales during parasitic beam tests in Hall A in upcoming 12 GeV experiments, and thus to confirm that the required stability and resolution are achievable.

5. EXPECTED RESULTS

The expected statistical uncertainty on the ^{3}He single-target PVDIS asymmetry is shown in Fig. 8. These are the same uncertainties as Fig. 7 but we include only results using the $Q^2 > 3$ (GeV/c)^2 trigger cut here. As one can see, the combined statistical uncertainties are as low as (9-10)% for the four x bins between 0.25 and 0.45, and are $< 20\%$ for a wide $x = (0.2, 0.75)$ range.

To estimate the impace on the understanding of the nucleon spin and the polarized PDF, the
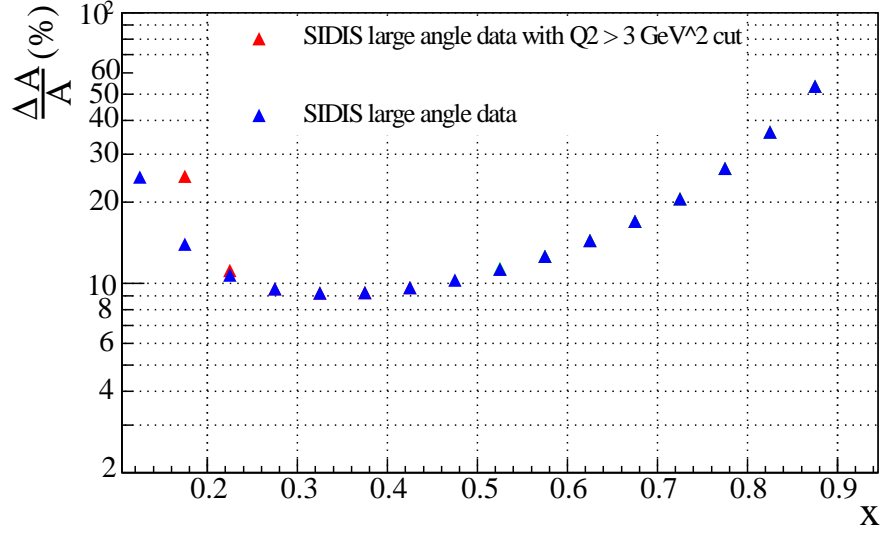
FIG. 8: Expected statistical uncertainty on the ^{3}He single-target PVDIS asymmetry, $\Delta A_{3He}/A_{3He}$ in percent, for the large-angle detector package of SoLID using a $Q^2 > 3\,(\text{GeV}/c)^2$ trigger cut. Data from different Q^2 bins were combined to reduce the statistical uncertainty.

JAM Collaboration [23] have been working on performing fits without the SU(3) constraint, and studying possible impact from the proposed measurement. Preliminary results show that the most impact is on the uncertainty of the polarized strange quark distribution, Δs, in particular in the $x = (0.2, 0.45)$ region where the proposed measurement has the most precision. Unfortunately, we were not able to reach a quantitative result by the submission deadline of this Letter. A reliable evaluation would require running the full JAM15 fit without the SU(3) constraint. It is also somewhat uncertain how a fit can be performed without the SU(3) constraint and without the new data, since in principle the fit is not solvable without a third condition. The collaboration is planning to continue this study, and may invest significant effort to sort out these questions if we proceed with a full proposal.

6. BEAM TIME AND NEW EQUIPMENT REQUEST

We request 180 PAC days of beam time for the main DIS production measurement. Additional time may be needed for systematic checkout, detector calibrations, and control measurements. Possible control measurements include measurements of beam-transverse asymmetries, tracking and PID studies at low beam currents. Significant configuration time may be needed for reversing

the target spin direction every minute. These details will be worked out if we move forward with the proposed measurement.

The experimental setup of the proposed measurement is very similar to the two approved SoLID SIDIS experiments using the polarized ^{3}He target, E12-10-006 [12] and E12-11-007 [13]. Therefore setup and installation time can be minimized if the measurement is scheduled adjacent to any of these two experiments. On the other hand, we do require the use a a new equipment, the polarized ^{3}He target with $16\times$ higher density compare to the planned stage-II upgrade for the GEn-II experiment. The density upgrade will require significant R&D. The Univ. of Virginia polarized ^{3}He group is planning to lead the target R&D with the aid of the polarized ^{3}He lab at JLab. However, we cannot estimate the additional installation time needed for the new target. This will be one more detail that will be worked out if we move forward with a full proposal.

7. SUMMARY

In summary, we propose here the first measurement of a parity-violating asymmetry between an unpolarized electron beam and a longitudinally polarized ^{3}He target in the deep inelastic scattering (DIS) region. The planned SoLID spectrometer in Hall A will be used along with a 60-μA, 11 GeV beam and a high-density polarized ^{3}He target. The polarized ^{3}He target will build upon the currently planned stage-II upgrade for the 12 GeV GEn experiment, with a further factor of 16 increase in the target density. This density upgrade can be done by increasing the fill pressure of the target cell by a factor 4, from 10 atm to 40 atm at the STP, and by holding the target chamber of the cell at the liquid nitrogen temperature. Using 180 PAC days, we will measure the ^{3}He single-target PVDIS asymmetry in the range $x = (0.20, 0.75)$, and achieve a sub-10% measurement in the four x bins between $x = (0.25, 0.45)$. The physics goal of the measurement will be three-fold: First, this will be the first measurement of the polarized electroweak interference structure functions $g_{1,5}^{\gamma Z}$. Secondly, the $g_1^{\gamma Z}$ is approximately proportional to $\Delta\Sigma \equiv \sum_f (\Delta q + \Delta\bar{q})$ (the approximation is valid if taking $\sin^2\theta_W = 0.25$, a value not too different from the actual 0.235). The proposed measurement will therefore provide direct, model-independent information on $\Delta\Sigma$, the quark spin contribution to the proton spin. Thirdly, by combining the extracted $g_1^{\gamma Z}$ with data on $g_1^{p,n}$ from double-polarization (spin structure) experiments, the SU(3) flavor symmetry can be tested for the first time. Moreover, the proposed measurement will serve as an expoloratory step

for the $g_{1,5}^{\gamma Z}$ measurement planned for the future electron-ion collider (EIC).

Acknowledgment

APPENDIX A: FORMALISM OF POLARIZED PVDIS

1. Formalism

For an unpolarized electron beam, the cross section different between scattering off a target with spin parallel and that with spin anti-parallel to the beam direction is [see Eq. (2.2.22) of Ref. [1]]:

$$
\frac{d^2\sigma^{\Rightarrow}}{dx\,dy} - \frac{d^2\sigma^{\Leftarrow}}{dx\,dy} \approx 16\pi M E \frac{\alpha^2}{Q^4} \left\{ (1-y)\left[g_V \eta^{\gamma Z}(g_3^{\gamma Z} - g_4^{\gamma Z}) + g_A^2 \eta^Z (g_3^Z - g_4^Z) \right] \right.
$$
$$
\left. + xy^2 \left[g_V \eta^{\gamma Z} g_5^{\gamma Z} + g_A^2 \eta^Z\, g_5^Z \right] + xy(2-y)g_A \eta^{\gamma Z} g_1^{\gamma Z} \right\}, \tag{A1}
$$

where for electron scattering, $g_V = g_V^e = -\frac{1}{2} + 2\sin^2\theta_W$ and $g_A = g_A^e = -\frac{1}{2}$. (For positron scattering, one only need to replace g_A^e by $g_A^{e^+} = -g_A^e$ in the equation above.) Other variables involved are

$$
\eta^\gamma = 1 \tag{A2}
$$
$$
\eta^{\gamma Z} = \left(\frac{G_F M_Z^2}{2\sqrt{2}\pi\alpha} \right) \left(\frac{Q^2}{Q^2 + M_Z^2} \right), \tag{A3}
$$
$$
\eta^Z = \left(\eta^{\gamma Z} \right)^2 \tag{A4}
$$

with $G_F = 1.166 \times 10^{-5}$ (GeV)$^{-2}$, $M_Z = 91.2$ GeV, $\frac{G_F M_Z^2}{2\sqrt{\pi}\alpha(Q^2+M_Z^2)} \approx \frac{G_F}{2\sqrt{2}\pi\alpha} \approx 180$ ppm and thus $\eta^{\gamma Z} = Q^2 \times 180$ ppm/(GeV)^2.

In the naive parton model, the structure functions involved on the RHS of Eq.(A1), as well as other frequently used ones, are

$$
F_1^\gamma = \frac{1}{2}\sum_f e_{q_f}^2 (q_f + \bar{q}_f) \qquad F_2^\gamma = 2xF_1^\gamma \tag{A5}
$$

$$
g_1^\gamma = \frac{1}{2}\sum_f e_{q_f}^2 (\Delta q_f + \Delta\bar{q}_f) \qquad g_2^\gamma = 0 \tag{A6}
$$

where $q_f = u, d, s, c$ the parton distribution density for flavor f. The γZ interference structure

functions are:

$$F_1^{\gamma Z} = \sum_f e_{q_f}(g_V)_{q_f}(q_f + \bar{q}_f) \qquad F_2^{\gamma Z} = 2xF_1^{\gamma Z} \tag{A7}$$

$$F_3^{\gamma Z} = 2\sum_f e_{q_f}(g_A)_{q_f}(q_f - \bar{q}_f) \tag{A8}$$

$$g_1^{\gamma Z} = \sum_f e_{q_f}(g_V)_{q_f}(\Delta q_f + \Delta\bar{q}_f) \tag{A9}$$

$$g_2^{\gamma Z} = g_4^{\gamma Z} = 0 \tag{A10}$$

$$g_5^{\gamma Z} = \sum_f e_{q_f}(g_A)_{q_f}(\Delta q_f - \Delta\bar{q}_f) \qquad g_3^{\gamma Z} = 2xg_5^{\gamma Z} \ . \tag{A11}$$

And the purely-weak interaction structure functions are :

$$F_1^Z = \frac{1}{2}\sum_f (g_V^2 + g_A^2)_{q_f}(q_f + \bar{q}_f) \qquad F_2^Z = 2xF_1^Z \tag{A12}$$

$$F_3^Z = 2\sum_f (g_V g_A)_{q_f}(q_f - \bar{q}_f) \tag{A13}$$

$$g_1^Z = \frac{1}{2}\sum_f (g_V^2 + g_A^2)_{q_f}(\Delta q_f + \Delta\bar{q}_f) \tag{A14}$$

$$g_2^Z = -\frac{1}{2}\sum_f (g_A^2)_{q_f}(\Delta q_f + \Delta\bar{q}_f) \tag{A15}$$

$$g_5^Z = \sum_f (g_V g_A)_{q_f}(\Delta q_f - \Delta\bar{q}_f) \qquad g_3^Z = 2xg_5^Z \tag{A16}$$

$$g_4^Z = 0 \ . \tag{A17}$$

The weak neutral couplings for the electron and quarks can be calculated using

$$\sin^2\theta_W = 0.232 \ ,$$

which gives

$$g_V^e = -\frac{1}{2} + 2\sin^2\theta_W = -0.036 \tag{A18}$$

$$g_V^u = \frac{1}{2} - \frac{4}{3}\sin^2\theta_W = 0.191 \tag{A19}$$

$$g_V^d = -\frac{1}{2} + \frac{2}{3}\sin^2\theta_W = -0.345 \tag{A20}$$

$$g_V^s = -\frac{1}{2} + \frac{2}{3}\sin^2\theta_W = -0.345 \tag{A21}$$

And the axial couplings are

$$g_A^e = -\frac{1}{2}, \quad g_A^u = \frac{1}{2}, \quad g_A^d = -\frac{1}{2}, \quad g_A^s = -\frac{1}{2} \tag{A22}$$

2. Medium-Energy Approximations

At $Q^2 \ll M_Z^2$, $\eta^Z \ll \eta^{\gamma Z}$ [Eqs.(A3,A4)] and the pure-weak terms can be safely neglected. Also note $g_4^{\gamma Z, Z} = 0$ in the parton model. We have

$$\frac{d^2\sigma^{\Rightarrow}}{dx\,dy} - \frac{d^2\sigma^{\Leftarrow}}{dx\,dy} \approx 16\pi ME\frac{\alpha^2}{Q^4}\left[(1-y)g_V\eta^{\gamma Z}g_3^{\gamma Z}\right.$$
$$\left.+xy^2 g_V\eta^{\gamma Z}g_5^{\gamma Z} + xy(2-y)g_A\eta^{\gamma Z}g_1^{\gamma Z}\right] . \tag{A23}$$

In the following we expand $g_{1,3}^{\gamma Z}$ for the proton and the neutron using Eqs. (A18-A22). Neglecting heavy flavors t, b, we have for the proton:

$$g_1^{p,\gamma Z} = \frac{2}{3}\left(\frac{1}{2} - \frac{4}{3}\sin^2\theta_W\right)(\Delta u + \Delta\bar{u} + \Delta c + \Delta\bar{c})$$
$$-\frac{1}{3}\left(-\frac{1}{2} + \frac{2}{3}\sin^2\theta_W\right)(\Delta d + \Delta\bar{d} + \Delta s + \Delta\bar{s}) \tag{A24}$$
$$\approx \frac{1}{9}\left(\Delta u + \Delta\bar{u} + \Delta c + \Delta\bar{c} + \Delta d + \Delta\bar{d} + \Delta s + \Delta\bar{s}\right) \tag{A25}$$

where the approximation is valid if we take $\sin^2\theta_W \approx 0.25$. And for the neutron:

$$g_1^{n,\gamma Z} = \frac{2}{3}\left(\frac{1}{2} - \frac{4}{3}\sin^2\theta_W\right)(\Delta d + \Delta\bar{d} + \Delta s + \Delta\bar{s})$$
$$-\frac{1}{3}\left(-\frac{1}{2} + \frac{2}{3}\sin^2\theta_W\right)(\Delta u + \Delta\bar{u} + \Delta c + \Delta\bar{c}) \tag{A26}$$
$$\approx \frac{1}{9}\left(\Delta u + \Delta\bar{u} + \Delta c + \Delta\bar{c} + \Delta d + \Delta\bar{d} + \Delta s + \Delta\bar{s}\right) \tag{A27}$$
$$\approx g_1^{p,\gamma Z} \tag{A28}$$

The $g_5^{\gamma Z}$ interference structure functions in the medium-energy regime become:

$$g_5^{p,\gamma Z} = \left[\frac{2}{3}\left(\frac{1}{2}\right)(\Delta u - \Delta\bar{u} + \Delta c - \Delta\bar{c}) - \frac{1}{3}\left(-\frac{1}{2}\right)(\Delta d - \Delta\bar{d} + \Delta s - \Delta\bar{s})\right] \tag{A29}$$
$$= \left[\frac{1}{3}(\Delta u_V + \Delta c - \Delta\bar{c}) + \frac{1}{6}(\Delta d_V + \Delta s - \Delta\bar{s})\right] \tag{A30}$$
$$g_5^{n,\gamma Z} = \left[\frac{1}{3}(\Delta d_V + \Delta s - \Delta\bar{s}) + \frac{1}{6}(\Delta u_V + \Delta c - \Delta\bar{c})\right] . \tag{A31}$$

The polarized PVDIS asymmetry is thus valuable in two ways: First, the dominant $g_1^{\gamma Z}$ term will provide complementary information on the polarized PDF to traditional spin structure experiments. Compared to semi-inclusive DIS measurements, using unpolarized beam DIS from polarized targets can avoid dealing with hadron fragmentations and thus can provide cleaner information. Moreover, the $g_5^{\gamma Z}$ term can be used to extract polarized valence quark polarization Δu_V and Δd_V, that

cannot be measured directly in traditional experiments. If we use existing knowledge on $\Delta u, d_V$, it is possible to isolate the polarized sea quark asymmetry $\Delta s - \Delta \bar{s}$ that cannot be measured at all in traditional spin structure experiments. In accessing $\Delta s - \Delta \bar{s}$, either the proton or the neutron data would be sufficient, in contrast to measurements of Δu and Δd where flavor decomposition requires data from both nucleons.

3. Polarized PVDIS Asymmetries

To calculate the size of the polarized PVDIS asymmetry, we devide Eq.(A1) by the sum of the two polarized cross sections, which equals to twice the unpolarized cross section. For the unpolarized cross section we can use either Eq. (9.23) on *p.*195 of Ref. [28] or Eq. (2.1.14) and (2.2.13) of Ref. [1], which are identical (checked this term-by-term). However to gain an intuitive idea of how the asymmetry is like, it is more convenient to ignore the term Mxy/E and use Eq. (9.24) of Ref. [28]:

$$\left(\frac{d^2\sigma}{dxdy}\right)_{\text{unpol}} = \frac{2\pi\alpha^2}{Q^4}s\left[1+(1-y)^2\right]\sum_f e_{q_f}^2 xq_f(x) \tag{A32}$$

$$= \frac{4\pi\alpha^2 ME}{Q^4}\left[1+(1-y)^2\right]\sum_f e_{q_f}^2 xq_f(x) \tag{A33}$$

where $s = 2k\cdot p = 2ME$ is used for fixed target scatterings. The asymmetry can thus be calculated as

$$A_{\text{pol-pvdis}} = \frac{\frac{d^2\sigma^{\Rightarrow}}{dx\,dy} - \frac{d^2\sigma^{\Leftarrow}}{dx\,dy}}{2\left(\frac{d^2\sigma}{dxdy}\right)_{\text{unpol}}} \tag{A34}$$

With the medium-energy approximation:

$$A_{\text{pol-pvdis}} \approx \eta^{\gamma Z}\frac{2xy(2-y)g_A g_1^{\gamma Z} + (2-2y+y^2)g_V g_3^{\gamma Z}}{[1+(1-y)^2]\sum_f e_{q_f}^2 xq_f(x)} \tag{A35}$$

$$= \eta^{\gamma Z}\frac{2x\frac{1-(1-y)^2}{1+(1-y)^2}g_A g_1^{\gamma Z} + g_V g_3^{\gamma Z}}{\sum_f e_{q_f}^2 xq_f(x)}. \tag{A36}$$

The structure of Eq. (A36) is quite special: First, the y-dependence appears in the $g_A^e g_V^q$ ($g_1^{\gamma Z}$) term. In other words the electron's parity-violating term is kinematically suppressed. This is opposite to the PVDIS asymmetry measured using a polarized beam and an unpolarized target, where the

quark parity-violation $g_V^e g_A^q$ ($F_3^{\gamma Z}$) term is kinematically suppressed. Secondly, the $g_A^e g_V^q$ ($g_1^{\gamma Z}$) term is still the dominant term of the asymmetry because of the small value of g_V^e. Third, the size of $A_{\mathrm{pol-pvdis}}$ is already smaller than A_{pvdis} because of the suppression from quark polarization ($\Delta q/q$). These features of Eq. (A36) make the size of $A_{\mathrm{pol-pvdis}}$ even smaller. Measuring $A_{\mathrm{pol-pvdis}}$ is thus much more difficult than the unpolarized-target PVDIS asymmetries.

---

[1] M. Anselmino, A. Efremov and E. Leader, Phys. Rept. **261**, 1 (1995) [Erratum-ibid. **281**, 399 (1997)] [arXiv:hep-ph/9501369].

[2] D. Wang *et al.* [PVDIS Collaboration], Nature **506**, no. 7486, 67 (2014). doi:10.1038/nature12964

[3] D. Wang *et al.*, Phys. Rev. C **91**, no. 4, 045506 (2015) doi:10.1103/PhysRevC.91.045506 [arXiv:1411.3200 [nucl-ex]].

[4] X. Ji and Y. Zhao, Int. J. Mod. Phys. Conf. Ser. **40**, 1660001 (2016). doi:10.1142/S2010194516600016

[5] J. P. Chen, A. Deur, S. Kuhn and Z. E. Meziani, J. Phys. Conf. Ser. **299**, 012005 (2011). doi:10.1088/1742-6596/299/1/012005

[6] F. Myhrer and A. W. Thomas, J. Phys. G **37**, 023101 (2010) doi:10.1088/0954-3899/37/2/023101 [arXiv:0911.1974 [hep-ph]].

[7] S. D. Bass and A. W. Thomas, Phys. Lett. B **684**, 216 (2010) doi:10.1016/j.physletb.2010.01.008 [arXiv:0912.1765 [hep-ph]].

[8] JLab 12 GeV G_E^n-II proposal, "Measurement of the Neutron Electromagnetic Form Factor Ratio G_E^n/G_M^n at High Q^2", B. Wojtsekhowski, G.D. Cates, spokespeople, (2009). URL: http://hallaweb.jlab.org/collab/PAC/PAC34/PR-09-016-gen.pdf

[9] M. Romalis, "Laser Polarized ^{3}He Target Used for a Precision Measurement of the Neutron Spin Structure", Ph.D. thesis, Princton University (1997).

[10] Z. E. Meziani *et al.*, Phys. Rev. Lett. **69**, 41 (1992). doi:10.1103/PhysRevLett.69.41

[11] Solid Pre-conceptual Design Report: http://hallaweb.jlab.org/12GeV/SoLID/download/doc/

[12] 12 GeV SoLID E12-10-006, "Target Single Spin Asymmetry in SIDIS $(e, e'\pi^\pm)$ Reaction on a Transversely polarized ^{3}He Target at 11 GeV", H. Gao, X. Qian, X.D. Jiang, J.-C. Peng, spokespeople; URL: http://hallaweb.jlab.org/collab/PAC/PAC34/PR-09-014-transversity.pdf

[13] 12 GeV SoLID E12-11-007, "Asymmetries in SIDIS $(e, e'\pi^\pm)$ Reactions on a Longitudinally Po-

larized ^{3}He Target at 8.8 and 11 GeV", J.-P. Chen, Y. Qiang, J. Huang, spokespeople; URL: https://www.jlab.org/exp_prog/PACpage/PAC37/proposals/Proposals/New Proposals/PR-11-007.pdf

[14] Kondo Gnanvo, Xinzhan Bai, Chao Gu, Nilanga Liyanage, Vladimir Nelyubin, Yuxiang Zhao, NIM. A 808 (2016) 83-92

[15] https://gemc.jlab.org/

[16] A. Buckley, J. Ferrando, S. Lloyd, K. Nordstrm, B. Page, M. Rfenacht, M. Schnherr and G. Watt, Eur. Phys. J. C **75**, 132 (2015) doi:10.1140/epjc/s10052-015-3318-8 [arXiv:1412.7420 [hep-ph]].

[17] E. R. Nocera *et al.* [NNPDF Collaboration], Nucl. Phys. B **887**, 276 (2014) doi:10.1016/j.nuclphysb.2014.08.008 [arXiv:1406.5539 [hep-ph]]. Source code can be downloaded from: https://nnpdf.hepforge.org/html/nnpdfpol10/nnpdfpol10sets.html

[18] E. Leader, A. V. Sidorov and D. B. Stamenov, Phys. Rev. D **82**, 114018 (2010) [arXiv:1010.0574 [hep-ph]].

[19] J. Bluemlein and H. Bottcher, Nucl. Phys. B **636**, 225 (2002) [arXiv:hep-ph/0203155].

[20] D. de Florian, R. Sassot, M. Stratmann and W. Vogelsang, Phys. Rev. Lett. **101**, 072001 (2008) [arXiv:0804.0422 [hep-ph]].

[21] D. de Florian, R. Sassot, M. Stratmann and W. Vogelsang, Phys. Rev. D **80**, 034030 (2009) [arXiv:0904.3821 [hep-ph]].

[22] A. Accardi, L. T. Brady, W. Melnitchouk, J. F. Owens and N. Sato, arXiv:1602.03154 [hep-ph].

[23] N. Sato *et al.* [Jefferson Lab Angular Momentum Collaboration], Phys. Rev. D **93**, no. 7, 074005 (2016) doi:10.1103/PhysRevD.93.074005 [arXiv:1601.07782 [hep-ph]].

[24] X. Zheng *et al.* [Jefferson Lab Hall A Collaboration], Phys. Rev. Lett. **92**, 012004 (2004) doi:10.1103/PhysRevLett.92.012004 [nucl-ex/0308011].

[25] X. Zheng *et al.* [Jefferson Lab Hall A Collaboration], Phys. Rev. C **70**, 065207 (2004) doi:10.1103/PhysRevC.70.065207 [nucl-ex/0405006].

[26] J. Gao and P. Nadolsky, JHEP **1407**, 035 (2014) doi:10.1007/JHEP07(2014)035 [arXiv:1401.0013 [hep-ph]].

[27] D. Wang *et al.* [Jefferson Lab Hall A Collaboration], Phys. Rev. Lett. **111**, no. 8, 082501 (2013) doi:10.1103/PhysRevLett.111.082501 [arXiv:1304.7741 [nucl-ex]].

[28] Halzen and Martin, "Quark and Leptons".